FUKUSHIMA CORE MELT COMPOSITION SIMULATION WITH ASTEC

H. Bonneville, L. Carénini and M. Barrachin
Institut de Radioprotection et de Sûreté Nucléaire (IRSN)
31, avenue de la division Leclerc, Fontenay-aux-Roses, 92260, FRANCE
herve.bonneville@irsn.fr; laure.carenini@irsn.fr; marc.barrachin@irsn.fr

ABSTRACT

IRSN used the ASTEC code to perform numerical simulations of the Fukushima-Daiichi accidents in the frame of the OECD BSAF project. Presently, simulations are available for the three units and for six days from the earthquake. A clear lesson from the project phase 1 was that the uncertainties on the safety systems functioning and accident progression are still large and many ways are liable to explain the measured thermo-hydraulics behavior. Rather than focusing on the thermo-hydraulics key-parameters for which comparisons with measurements are available, the presentation will address melt composition computation results which may provide insights relevant for the decommissioning process.
When the molten corium relocates from the core down to the vessel lower head, the melt jets interact with water and may be totally or partially fragmented depending on the level of water. A U–Zr–O–Fe molten pool may form in the lower head and due to chemical reactions, separation between non-miscible metallic and oxide phases may occur. The models implemented in ASTEC enable to simulate these phenomena. Up to five different axisymmetric corium layers in the vessel bottom head can be formed, which are, from bottom to top: a debris layer, a heavy metallic layer, an oxide layer, a light metallic layer and another debris layer. An important process is the UO_2 fuel reduction to metallic uranium by non-oxidized zirconium which results in uranium transport to the dense metallic layer as demonstrated in the MASCA Program.
Complex melt compositions before vessel failure will be presented for the current “best-estimate” cases with a special focus on Unit 1 due to the large consensus on the accident progression for this Unit.
It should be underlined that in case of vessel bottom failure a part of this complex melt will be relocated to the pedestal and a molten core concrete interaction will take place enhancing other complex physical phenomena with possible large consequences on the melt chemical composition and behavior.

KEYWORDS
Fukushima-Daiichi, ASTEC, simulation, melt composition

1. INTRODUCTION

To get a more precise idea of the core melt composition after the severe accidents at the Fukushima-Daiichi power plant is important for preparing the reactor decommissioning. As such it was one of the challenges assigned to the Benchmark of the Severe Accidents at Fukushima-Daiichi (BSAF) phase 1 project [1]. To get such knowledge is a rather complex task due to the number of different materials present in the core and the vessel and their complex chemical interactions at high temperatures. The main materials involved are uranium dioxide (UO_2) for the fuel, zirconium (Zr) used for the fuel cladding and the fuel channel, boron carbide (B_4C) for the control rods and different varieties of steel, for control rods cladding and sheaths, and for the vessel.

Metallic uranium (U) is one of the metallic species which may form during the accident progression due to the presence of a miscibility gap between two liquids in the quaternary diagram U-Zr-Fe-O. This possibility was demonstrated during the MASCA experiments [2] in 2004 and numerical models were then developed to take such a reaction into account.
A model taking into account the formation of U in the lower head is implemented in the V2.0 version of the ASTEC code.

2. ASTEC MODELLING OF THE CORIUM BEHAVIOUR IN THE VESSEL LOWER PLENUM

2.1. The corium layers dynamics

In ASTEC V2.0 version the corium in the lower plenum may be stratified into a maximum of five layers as shown on Figure 1. below: two are constituted of solid debris and three of magma (name given to the melt in the ASTEC terminology). The number of the layers effectively present depends on the slump characteristics, the water mass in the lower head at the slump time and the nature of the materials in presence.

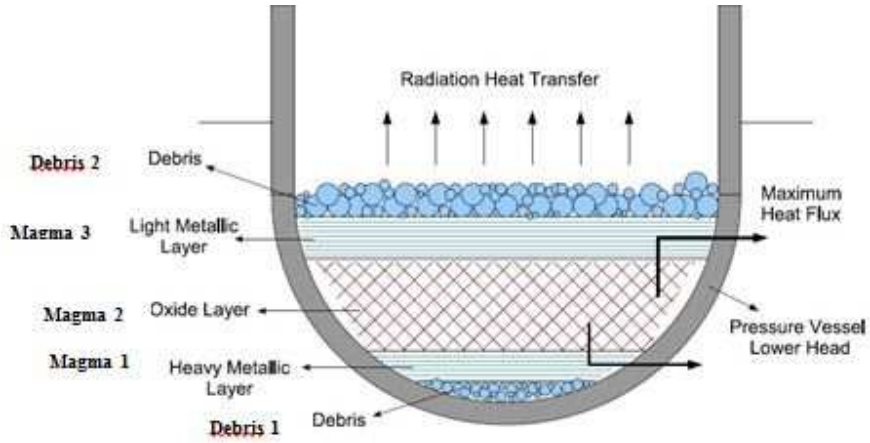

Figure 1. A typical debris configuration in lower plenum.

The debris are produced by the interaction of a melt jet with water present in the lower plenum. When the molten corium relocates from the core down to the lower plenum, the melt jets interact with water and may be totally or partially fragmented depending on the level of water inside the vessel. The code evaluates the jet break-up length and deduces the fragmentation rate and the associated water vaporization.
If the first melt jet is totally fragmented, a debris bed is created at the bottom of the lower plenum –this is the debris 1 layer in ASTEC terminology - but if it is only partially fragmented, a corium layer – magma 1 in ASTEC terminology - is formed at the bottom, covered by the debris bed – the debris 2 layer in ASTEC terminology. The corium which is in a magma layer can never join one of the debris layers whereas debris may melt and be incorporated to magma layers. The magma layer may split into up to three layers depending on the thermo-physical properties of the corium. This will be explained below. When a corium slump occurs in a lower head where a magma layer is already present, the debris due to the jet fragmentation will join the debris 2 layer and the magma the upper magma layer.
The rationale behind the magma phase separation lies in the miscibility gap in the liquid state between stainless steel and UO_2 and ZrO_2 refractory oxides. This leads to segregation of metallic and oxide phases formed in the dominant U-Zr-O-Fe quaternary mixture appearing in corium. When zirconium is fully

oxidized, it is usually expected that a lighter metal layer mainly composed of stainless steel will be formed on a heavier oxide UO_2-ZrO_2 layer. When zirconium is not fully oxidized, metallic zirconium is able to reduce UO_2 and enrichment in U may occur in the metallic phase. In a series of small and medium-scale tests performed in the OECD/NEA sponsored MASCA program with iron and stainless steel as additional material, a migration of metallic zirconium and uranium was effectively noticed from sub-oxidised corium towards the metallic phase (initially iron or steel), leading to the increase of metallic phase mass and density. The inversion of positioning of metal layer also sometimes leads to transitory formation of a lighter layer of molten metal on the top, as observed in some MASCA tests. This produces a molten pool having a three-layered structure (bottom-to-top): molten *heavy* metal - molten oxides - molten *light* metal, respectively magma 1, magma 2 and magma 3 layers in the ASTEC terminology. Thus a typical schematic representation of debris can be one as shown in figure 1. The formation of the layered structure dictates the heat transfer profile and focusing effect, thus, influences the thermal evolution, the mode and location of vessel failure, in case it occurs. The focusing effect is the concentration of the upward heat flux to the vessel sidewall through a thin metal layer laying above the oxide pool.
During the process the corium segregates into different phases, the phases migrate themselves into layered structures, the dynamics of which depends on their relative density and related dynamic effects. The overall process of phase separation is thus the result of interaction of thermochemical separation of phases and hydrodynamic formation of layered structures and this takes place in a sequence in the form of a multistep process. In the process of progression of the events, the quasi-separated (by virtue of complex interactions of different mechanisms outlined above) phases of corium get stacked in different layers, then each layer of quasi-phase-separated corium again undergoes phase separation. The process continues in synchronization with the dynamics of the accident progression.

2.2. The phase separation modelling

The steps involved in these models are:

1. decomposition of some of the reactor core materials in standard materials suitable for thermochemical phase separation modelling (steel for instance is split into Fe, Ni and Cr);
2. thermochemical phase separation models. The current phase separation model is based only on four elements U, Zr, O and Fe. The thermodynamic equilibrium in this mixture is searched by the minimization of Gibbs free energy of the system. Once the atomic composition of the two phases has been determined, the separated elements are recombined, first U and Zr with oxygen in the same proportion, than if oxygen is still available, oxygen with Fe to form FeO;
3. modeling of hydrodynamic separation of corium materials directly involved in thermochemical phase separation modelling and other materials present in the corium. The hydrodynamic separation depends on the density of the layers and the layer liquid fraction. There will be no phase separation when the layer liquid fraction is too low.

2.3. Validation against the MASCA experiments

The MASCA series of experiments, performed by NRC-KI (Russia), were designed to study the phase separation of mixtures of UO_2, ZrO_2, Zr and Fe/Steel under inert atmosphere. Some of the experiments also involved fission products simulants, namely Mo, Ru, Sr, Ba, Ce, La, in order to evaluate their re-distribution between the non-miscible phases. For more information, readers may refer to [2], [3] and [4].
The V2.0 version of ASTEC was used to simulate the 21 experiments of the MASCA program: 17 with 0.5 kg of mixture (STFM series) and 4 with 2 kg (MA series). For all the experiments, the ASTEC V2.0 predictions for corium separation in the presence of structural materials (Fe/Steel) and for fission products distributions are reasonably good and follow the trends observed. The relative errors in metallic mass predictions are on average of 21% for the STFM series (36% maximum) and of 12% for the MA series (21% maximum).

The limitation of this validation task is the transient behaviour of the separation (the mass transport between the layers is calculated by modelling migration of drops) which could not be assessed due to lack of experimental data. This will need further investigation in the frame of the CORDEB project (MASCA follow-up [5]), in particular regarding the impact of an oxidising atmosphere on the phase separation.

3. IN-VESSEL MELT COMPOSITION FOR UNIT 1

3.1. In-vessel accident progression (Degradation Phase)

Comparing to the situations in the two others Units, the situation of Unit 1 of Fukushima-Daiichi Nuclear Power Plant (1F1) has two specificities that have to be accounted for when starting the simulations:

1. the core water injection was interrupted for more than 15 hours which is largely sufficient for the core to melt down, to form a break in the lower head, to pour corium to the basemat and to initiate a Molten Core Concrete Interaction (MCCI),
2. very few measurements are available for comparison with the simulation results and understanding will remain partial until additional information is obtained from the plant decommissioning.

Based on Pressurized Water Reactor (PWR) experience at IRSN (there is no BWR operated in France), it was supposed that a vessel bottom head failure occurring when Reactor Pressure Vessel (RPV) pressure is above 7 MPa and inside a rather small containment (by comparison to PWR) would enhance the risk of Direct Containment Heating (DCH) that may lead to an important risk of failure of the containment. No such a situation is likely to have occurred in Unit 1 and a path for depressurization of the vessel has to be identified. A steam line rupture may be caused by creep due to the combination of pressure load (the vessel pressure is around 7 MPa) and thermal load (hot steam flows through the steam pipe when a SRV is cycling). The steam line rupture was predicted using a damage function based on a Larson-Miller Parameter (LMP) value for stainless steel. With the expression used no steam line rupture was predicted. However, creep tests show a wide dispersion of the results which must be taken into account by introducing corrective coefficients into the LMP expression. So a steam line rupture around 7 h after scram (March 11 21:43) was considered as a serious possibility and retained as a computation parameter. Giving the results closest to the few measurements, this test case is chosen as the best estimate computation.
With this last assumption, vessel failure occurs quite early in the night but after vessel has been depressurized. The containment pressure behavior can more or less be reproduced under the condition to activate different leaks. The first leak to be activated is the leak from the Dry Well (DW) to the refueling bay through the containment lid flange which is a “classical” leakage point for Mark I containment that is well identified and modeled. However, this leakage is not sufficient to explain the containment pressure behavior and some other leakages have to be assumed later on as highlighted below.
Figure 2. displays the computed water level (continuous blue line) and the measured points (red dots). Two measurement points only are available before March 11, 20:00. Comparison to both of them highlights the fact that the computed water level decrease is too fast. At the time they have been measured the water level measurements are reliable and show that the core is still under water. The only possible explanation seems to be that the initial water inventory is underestimated in the numerical model as water in the recirculation loops has not been taken into account. In the computation, the water level reaches the Top of Active Fuel assembly (TAF) 1h 38min after the scram (March 11 16:24) and the core is completely uncovered when the bottom of fuel assembly (BAF) is reached 3h 27min after scram (March 11 18:14). The vessel depressurization, due to the main steam line rupture 6h 56min after scram (March 11 21:43), causes a steam flashing and the water level falls to 1.5 m. Then 7h 9 min after scram (March 11 21:56), an important corium slump to the lower head (see chapter 3.2 on molten material plots) causes the vaporization of any remaining water. After this corium slump, the computed water level corresponds to

the upper level of the corium pool as the water mass inventory is residual. The vessel rupture occurs 10h 6 min after scram (March 12 0:51).
It has been demonstrated that the measurement points available after March 11 21:00 are not reliable due to the measurement technology based on a pressure difference.

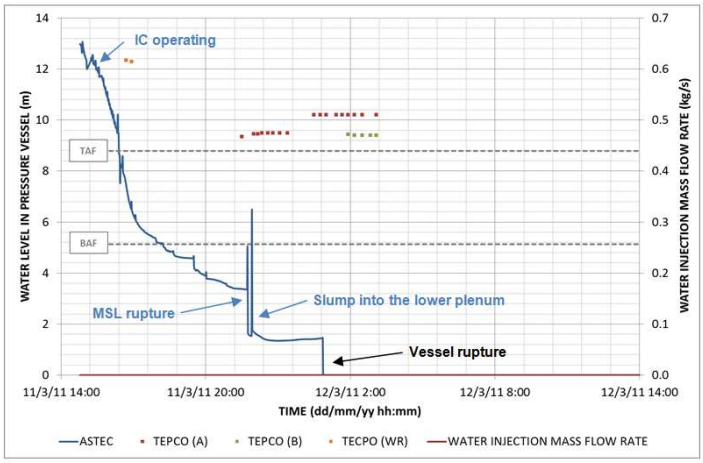

Figure 2. Water level in the vessel (m) - computed and measured values

The main steam line damage (Figure 3.- right) increases sharply when the gas temperature is above 1200 K although it is only a little above 5%, 6h 56 min after scram (March 11 21:43), which time was chosen to trigger the main steam line rupture. Considering the uncertainties in both the Larson-Miller parameter and the magma progression downwards this rupture hypothesis was considered as reliable. Before the MSL rupture the vessel pressure is around 70 bar regulated by the Steam Relief Valves (SRV) cycling. After the MSL rupture the vessel pressure is at equilibrium with the containment pressure at around 0.7 MPa. Results are not presented here as only two measurement points are available for comparison.

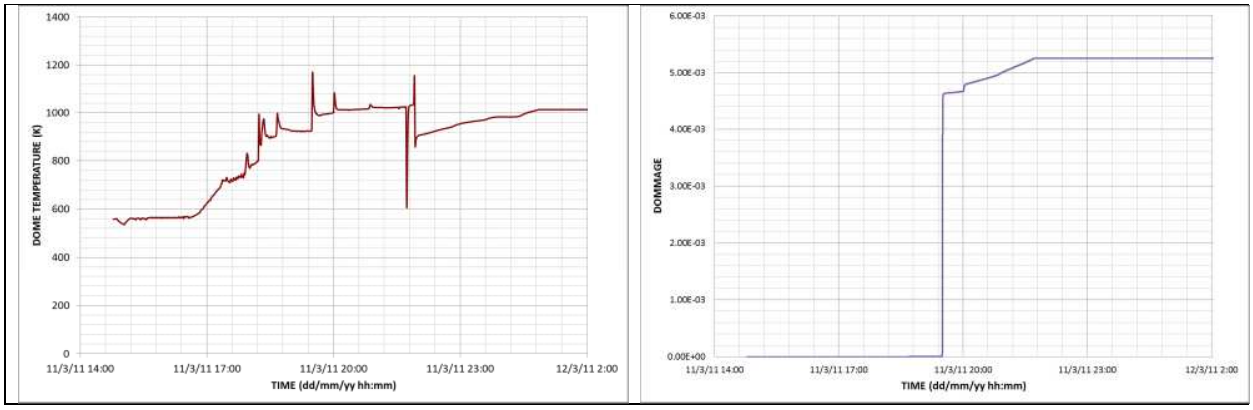

Figure 3. Gas temperature in the dome (left) – Damage on the main steam line

Figure 4. shows the corium mass relocated in the vessel bottom head (continuous red line) and the mass of magma (sum of molten materials and debris) in the core zone (continuous blue line). The melting of the core (ref. Molten material plots) starts around 2h 34min after the scram (March 11 17:20). The maximum of the magma mass before relocating in the lower head is equal to 110 000 kg. The significant corium slump (82 400 kg) to the lower head occurs 7h 9min after scram (March 11 21:56), involving the

vessel rupture around 3 hours after. The vessel head fails due to a ductile failure enhanced by a partial fusion of the bottom head wall (clearly visible on Figure 5, picture bottom right, near the centerline).

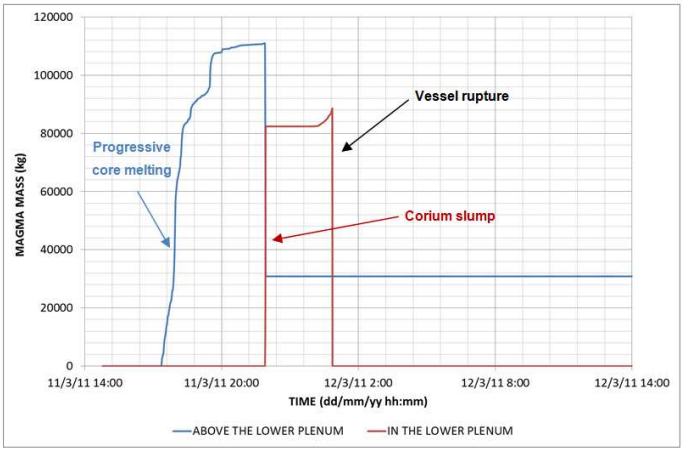

Figure 4. Mass of magma and slump to the lower head (kg)

It should be noted that after the vessel rupture, all the corium of the lower head is transferred in the cavity in the ASTEC modelling. However, due to uncertainties on core degradation after vessel rupture, the transfer kinetics of corium still in the core at vessel rupture is a parameter in the code that must be defined beforehand.

Progression of the molten/destroyed materials through the core may be clearly seen on the drawings below (Figure 5.) which give the temperature field inside the vessel at four different characteristic times (in second from the earthquake inside the yellow boxes on the upper side right): when TAF is reached (top left); just after the main steam line rupture (top right); at slump time just after main steam line rupture (bottom left); and at vessel bottom head failure (bottom right).

The dynamics of the magma layers in the bottom head may be appreciated by comparison of the two drawings at the bottom and by considering Figure 6. which shows the mass of each layer as a function of time.

1. On March 11, 22:00 (time 26000 s), three layers are clearly visible corresponding from bottom to top to a magma 2 layer, a magma 3 layer and a debris 2 layer. There is a small magma 1 layer but no visible due to its small mass.
2. On March 12, 0:51 (time 36280 s), only two layers may be distinguished corresponding to a magma 1 layer and a magma 3 layer. The debris present in the debris 2 layer have molten and the magma 2 materials have mostly moved to either the magma 1 layer or the magma 3 layer.

The first massive corium slump to the lower head occurs when the bottom head is still full of water causing a large fragmentation of the melt and the formation of a debris bed (around 20 tons) located above a large magma bed (around 60 tons). This debris bed will progressively be heated by its own residual power and by the heat exchanges with the magma layer below so that it is completely molten around March 11, 24:00.

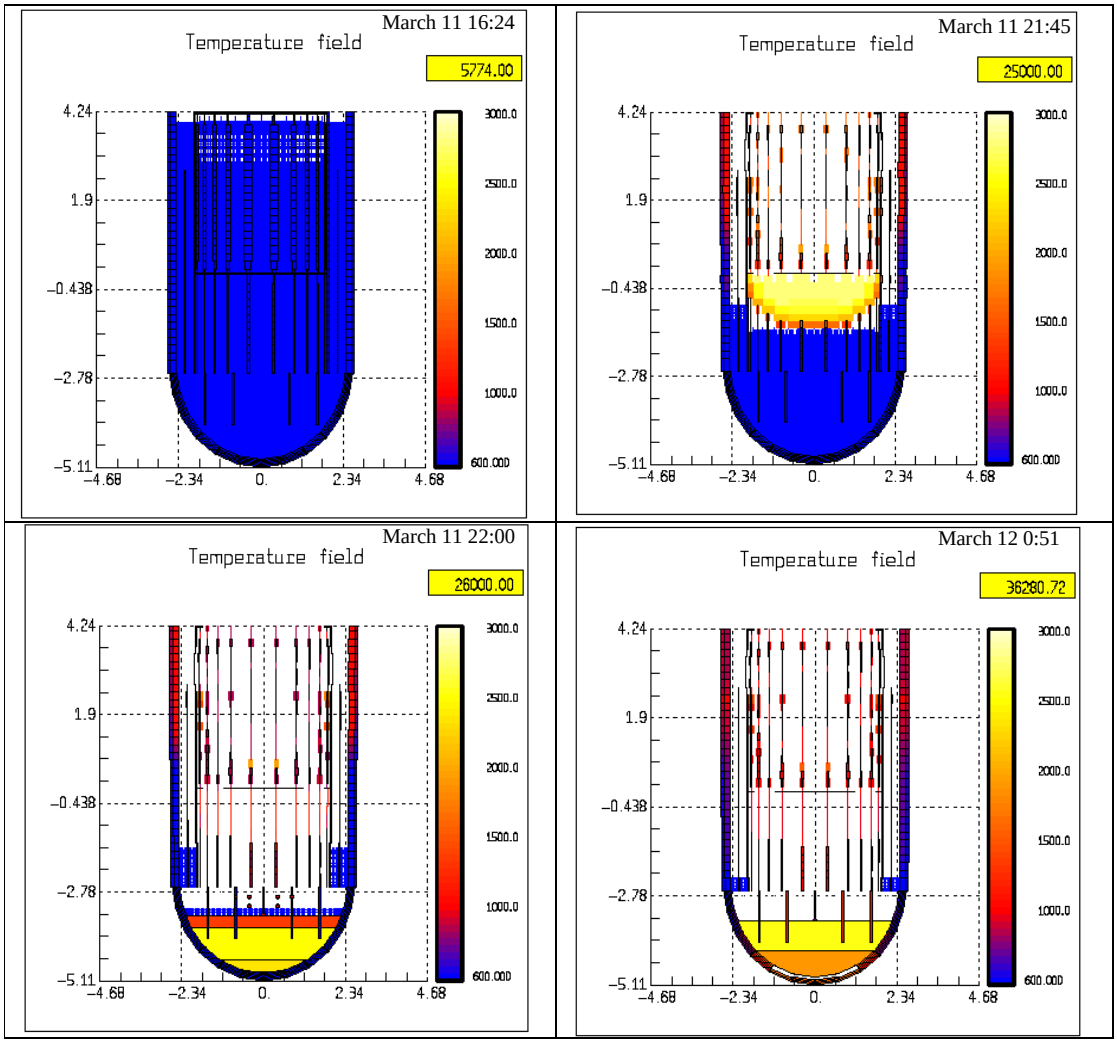

Figure 5. 1F1 - Degradation phase – location of the materials and temperature field for four characteristic times (top left: water at TAF – top right: main steam line rupture – bottom left: first major corium slump – bottom right: vessel failure)

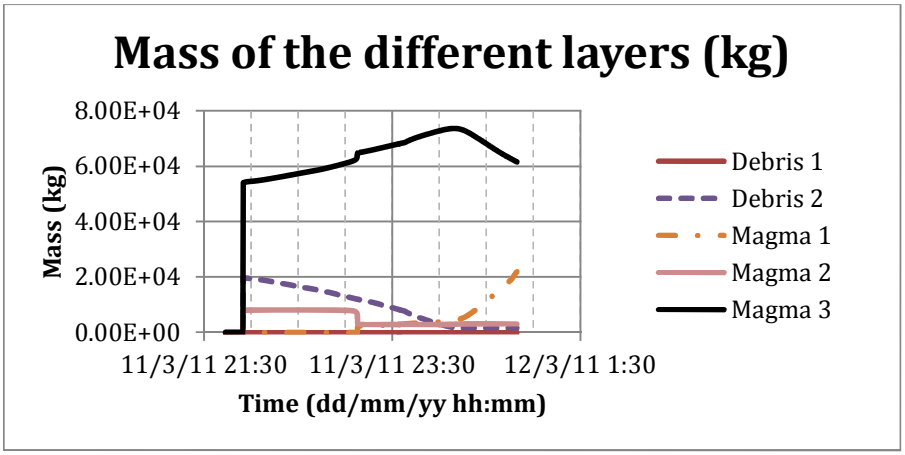

Figure 6. 1F1 - Evolution of the lower head corium layers mass with time

3.2. In-vessel melt composition for Unit 1

As may be seen on Figure 8. and Figure 9. essentially two layers are present at vessel failure time:

1. a molten heavy metal layer at the bottom consisting mainly of steel compounds issued mainly from the bottom head partial fusion under thermal load, of Zr, and metallic U,
2. a lighter mixture layer with a large diversity of materials due to the fact that at vessel failure the phase separation is still an on-going process.

The three figures below present - from the first slump to the calculated vessel failure, a) the total mass in the lower head (including the debris layer) of the species Zr, ZrO, ZrO_2, U and UO_2 (Figure 7.), b) the U and UO2 mass distribution in the three magma layers (Figure 8.), c) the Zr compounds and steel compounds distribution in the same three magma layers (Figure 9.). Table I below presents a short inventory of the materials distribution in the magmas at vessel failure.
ZrO may be formed during clad oxidation beside Zr02. It may slump to the lower but may not be formed in the lower head where it may be present only in a debris layer. As soon as it is transferred to a magma layer it is decomposed into Zr and O and the equilibrium model will recompose it into Zr and ZrO_2. So no ZrO remains after the debris layer total melting.
The metallic uranium U is produced mainly just after the slump (around 7 tons for a total final mass of 9.3 tons) but the layer liquid fraction is rather low so that it is kept mostly in the upper layer. As debris melting brings new materials to the magma layer 3 some 2 t more of U metal are formed. After debris bed melting is completed, the liquid fraction of the magma layer begins to increase and heavy metals begin to move downwards to form a heavy-metal at the bottom of the lower head. It should be noticed that the vessel failure is computed at the level of this layer and around 40 min after it appears. The fusion point is rather low for this layer components and its liquid state enhances very efficient convective heat exchanges take place whereas the upper large magma 3 layer is still rather “solid” with much less efficient heat exchanges.

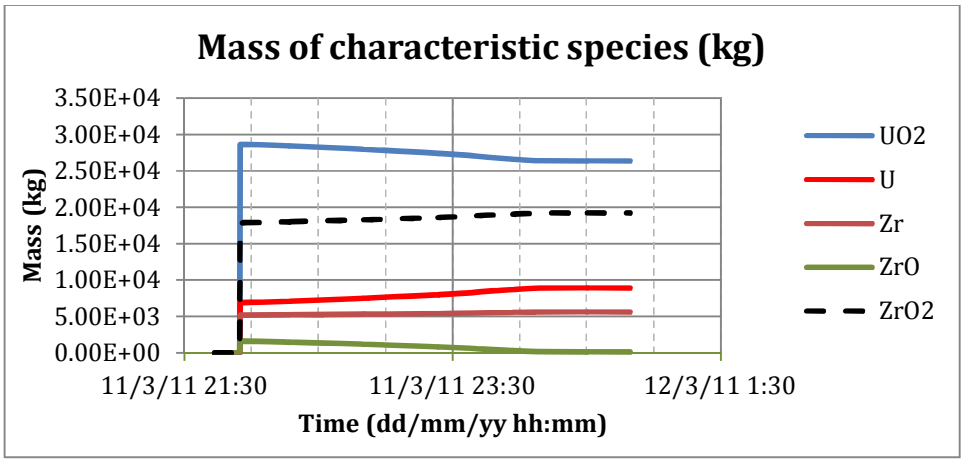

Figure 7. Unit 1 – Mass of characteristic species in the lower head

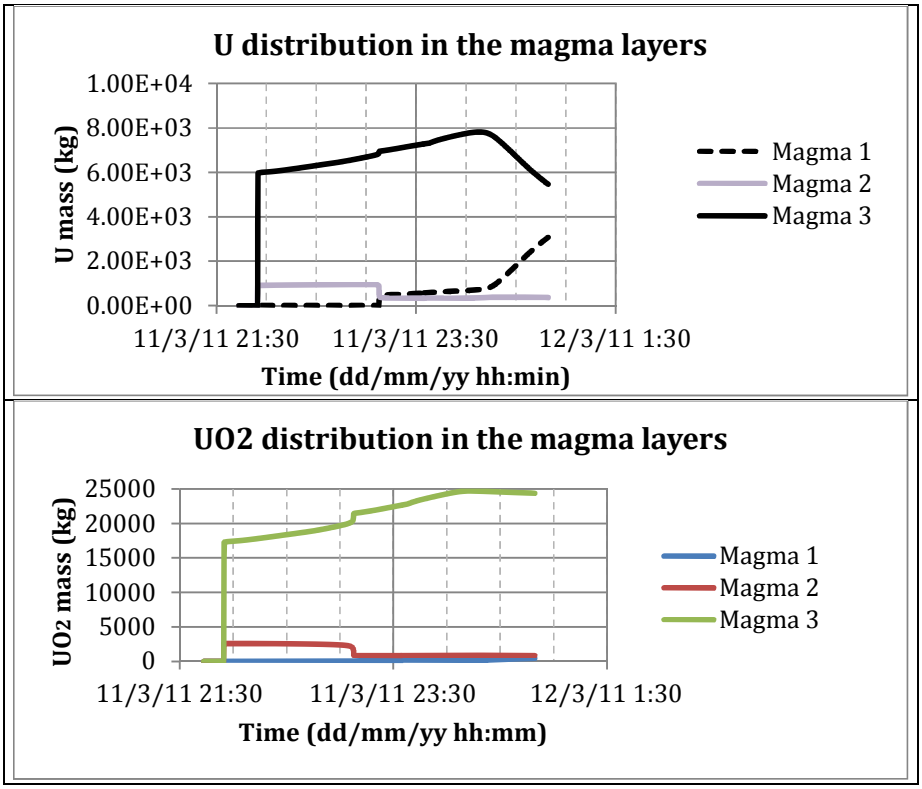

Figure 8. Unit 1 – Distribution of characteristic species in the magma layers (U and UO_2)

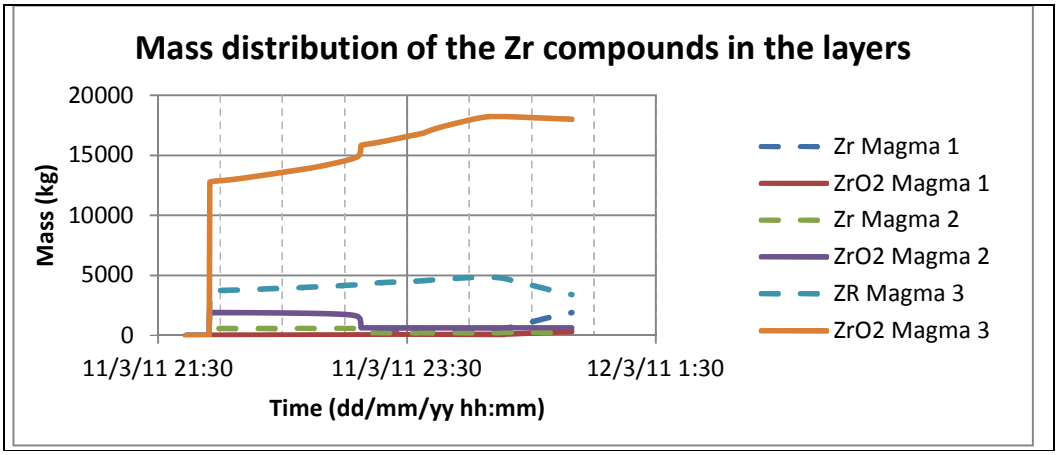

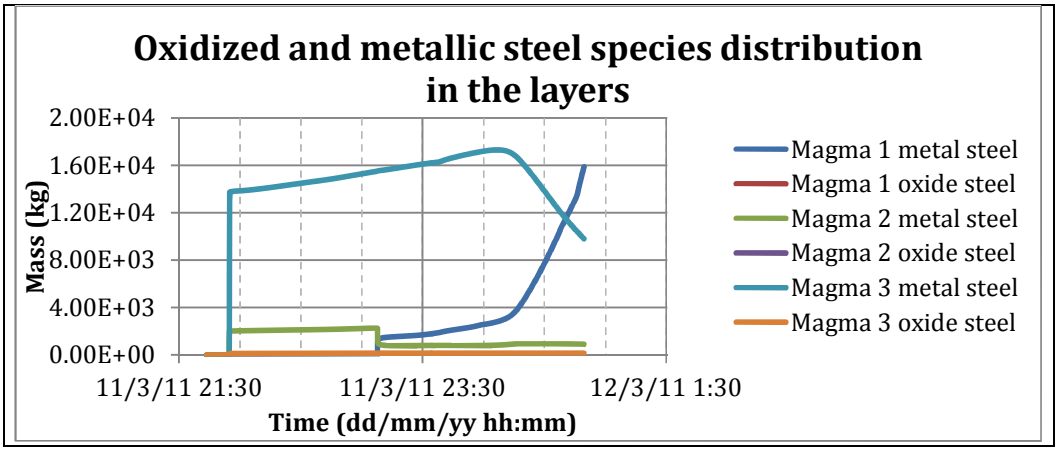

Figure 9. Unit 1 – Distribution of characteristic species in the magma layers (Zr and steel compounds)

At the time of vessel failure, the ratio between U present as a metal (9.3 tons) and the total mass of U in the magma layers (32.6 tons which includes the 23.3 tons bound in the 26.3 tons of UO_2) is more than 28 %, that is a rather large percentage. This large U mass is present in the three layers although mainly in the upper layer where it is formed and in the lower layer where it is progressively transferred due to its density It should be noticed that the vessel failure occurs whereas mass transfers between the layers are still taking place: the hydrodynamic equilibrium between corium layers has not yet been reached.

Table I. 1F1 – Main species distribution in the layers (kg/species/layer)

Species	U	UO_2	Zr	ZrO_2	B_4C	Steel	Oxidized steel species	Total
Magma 1	3080	427	1900	315	103	15900	< 3	22000
Magma 2	365	850	227	628	10	905	< 5	3010
Magma 3	5470	24300	3390	18000	104	9810	162	61500

This result has to be considered as indicative of metallic uranium presence in the corium. It must be said that chemical reactions associated involving B_4C are not taken into account in the ASTEC model. Boron is known to associate with Zr to form stable boride reducing so the possibility for Zr to reduce UO_2 to produce metallic uranium. Moreover, if metallic uranium has ever been present in the lower head, does it mean that one may expect to find some U during decommissioning operations ?

In case of Unit 1, it seems clear that most of the metallic uranium formed in the lower head slumped to the pedestal and was involved in the Molten Core Concrete Interaction (MCCI) taking place there. However, as large quantities of steam produced by the concrete erosion flows through the melt, it might be assumed that this metallic uranium has been re-oxidized, at least partially. In case of a corium stratification in the pedestal, one may expect a dense metal layer with U at the interface with concrete and more efficient concrete ablation as long as this layer remains, nevertheless uranium oxidation should occur in a few minutes.

An interesting point to notice is also the presence of a large mass of steel compounds coming for a large part from the partial fusion of the bottom head under the thermal loads.

4. IN-VESSEL MELT COMPOSITION FOR UNIT 2

For both Units 2 and 3, loss of water injection is long enough to cause important damage to the core as the decay heat is still around 10 MW but not sufficient to cause a vessel bottom head failure for which some more hours would be needed. So the main question to predict the core state after the first days of the

accident is to know what quantity of water was injected into the vessel in order to see if it is sufficient to re-flood the core and stop the core degradation progression or not.
What is roughly known in both cases is the total water mass which has been pumped to the core each day. With such a mass flow rate, the first ASTEC computations showed that the core was badly damaged but re-flooded so that no corium was poured to the pedestal. However the effectiveness of the water injections is rather uncertain and because of leaks on the injection lines only a percentage of the water injected may have effectively reached the core. For both units reference computations presented here were performed assuming only 15% of the water pumped to the core effectively reached it. This figure is based on initial BSAF recommendation assuming the vessels had effectively failed in both cases. What remains of the water mass flow rate is supposed to leak somewhere out of the containment.

4.1. In-vessel accident progression (Degradation Phase)

The simulation starts at 14:47 on March 11th at the instant of the reactor scram when the reactor is operating under nominal conditions i.e. the vessel pressure is 7 MPa as well and the water level is about 14.4 m.
After the tsunami, the RCIC operated by itself i.e. without any regulation from the operators, and highly probably out of its normal operating range. The steam turbine probably kept up functioning in two phase (that is liquid and steam phase) flow conditions which is rather unexpected. Still the consequence of this abnormal RCIC operation was that the water level was kept above the top of active fuel all the time. Then, the water level remains constant by the RCIC water injection. 69h 30min after the scram (March 14 12:15), the water level begins to fall due to the RCIC water injection decrease. The RCIC stops 69.7 h after scram (March 14 12:30). The top of active fuel (TAF) is reached 74.4 h after the scram (March 14 17:15). The core is totally uncovered one hour after. The water vaporization is enhanced by an important flashing when the operators succeeded in depressurizing the vessel.
A large molten pool is formed inside the core enabling an important corium slump into the lower plenum (141 000 kg) 84h 24min after scram (March 15 3:12), causing the vaporization of any remaining water in the lower head and involving the vessel rupture around 3 hours after (Figure 10. below). In the calculation, the vessel head fails due to a “fragile failure”. In the code terminology it corresponds to a damage based failure (i.e. failure is predicted when the damage reaches 1 anywhere along the meridian) and the damage rate is computed using a Kachanov model [6].

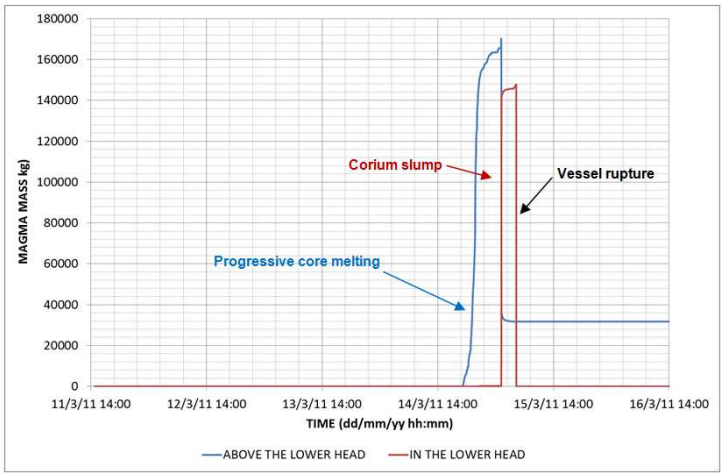

Figure 10. 1F2 - Mass of magma and slump into the lower plenum (kg)

4.2. In-vessel melt composition for Unit 2

The analysis for Unit 2 is limited to the presence of U. At vessel failure time 52.7 tons of UO_2 are located in lower head according to computations to be compared with 10.4 tons of U.
Due to the re-flooding operated the debris upper layer is not molten and rather significant with 63.7 tons consisting mainly of uranium dioxide, oxides of Zr (stoichiometric and non-stoichiometric) and stainless steel. The liquid layer composition is also more complicated than with Unit 1 as three layers are still present at the time of vessel rupture all of them with a significant weight: 14.3 t for the bottom magma 1 layer, 52.6 t for the middle magma 2 layer and 15.1 t for the upper magma 3 layer. Distribution of characteristic species in the layer at vessel failure time is displayed in Table II. below.

Table II. 1F2 – Main species distribution in the layers (kg/species/layer)

Species	U	UO_2	Zr	ZrO_2	B_4C	Steel species	Total
Magma 1	2960	400	1670	268	106	8896	14300
Magma 2	6590	16100	3700	10800	179	15231	52600
Magma 3	892	8010	503	5380	3	312	15100

In a whole, the quantity of metallic zirconium in the lower head is rather limited, only 6 tons of Zr quite similar to the 5.5 tons obtained for Unit 1 with much less materials slumped to the lower-head. The ratio between U present as a metal (10.4 tons) and the total mass of U in the magma layers (31.9 tons which includes the 21.5 tons bound in the 24.5 tons of UO_2) is approximately 32.6 % quite similar with the 28.0 % computed for Unit 1.
These results show the possibility that a significant mass of U was present in the vessel bottom head at a time. Similarly to Unit 1 in case of large vessel break and slump of most of this inventory to the pedestal, it may be assumed that the U was re-oxidized during the following MCCI. However, for Unit 2 as for Unit 3, the uncertainties on the degradation phase are large mainly due to the uncertainties on the water mass flow rate. A larger mass flow rate may increase the potential for Zr oxidation and so restrict the possibility of UO_2 reduction. On the other hand, a with a slightly more important water mass flow rate, most of the corium may still be located in the lower head. In such a case, the liquid phase would cool in bulk and oxidation of metallic U might be mainly by O diffusion through the solidified melt and so be rather slow leaving the possibility that metallic U is still present in the bottom head. Those considerations also hold true for Unit 3.

5. IN-VESSEL MELT COMPOSITION FOR UNIT 3

5.1. In-vessel accident progression (Degradation Phase)

The simulation started on March 11th 14:47 with the reactor scram. At this time the vessel pressure and the vessel water level are about their nominal operating conditions i.e. respectively 7 MPa and 14.4 m.
After reactor scram two safety systems were operated:

1. the Reactor Core Injection Cooling (RCIC) system is first set on according to the prescribed operating rules after the scram and was reset on after the tsunami (March 11 16:03). Steam is extracted from the vessel and exhausted to the wet-well water after having moved a steam turbine pumping water from the Injection Condenser (IC) to the vessel. This system failed down on March 12 11:36
2. the High Pressure Cooling Injection (HPCI) system after the RCIC failed down. It was set on March 12 12:35 and stopped by the operators – assuming it was no longer working correctly - on March 13 2:42.

The HPCI operation is rather difficult to assess precisely as the water level measurement was lost during the operation. The assumption which is made supposes the HPCI fails in two stages. First, the water injection stops 30h 18min after scram (March 12 21:00) whereas the steam extraction is stopped 35h 54min after scram (March 13 2:42). With these assumptions, the TAF is reached 35 h 51min after scram (March 13 2:39) and the core is totally uncovered 40h 18min after scram (March 13 7:02).
Loss of water injection is long enough to cause important damage to the core as the decay heat is still around 10 MW but not sufficient to cause a vessel bottom head failure for which some more hours would be needed. So the main question to predict the core state after the first days of the accident is to know what quantity of water was injected into the vessel in order to see if it is sufficient to re-flood the core and stop the core degradation progression or not.
What is roughly known is the total water mass which has been pumped to the core each day. The computations made with the assumption that all the water pumped to the core effectively reached the core showed that the core was badly damaged but re-flooded so that no corium was poured to the pedestal. However the effectiveness of the water injections is rather uncertain and leaks on the injection lines may have caused that only a percentage of the water injected reached the core.
A 15 % weighting coefficient has been applied to the mass flow rate injected in the vessel. What remains of the water mass flow rate is supposed to leak somewhere out of the containment. With this assumption, a large molten pool is formed in the core (Figure 11. below), enabling a first small corium slump into the lower plenum (4800 kg) 45h 6min after the scram (March 13 11:50) and a very large one (122 000 kg) 52h 42min after scram (March 13 19:27), involving the vessel rupture (in the calculation) around 6 hours after, 58h 48min after scram (March 14 1:36).

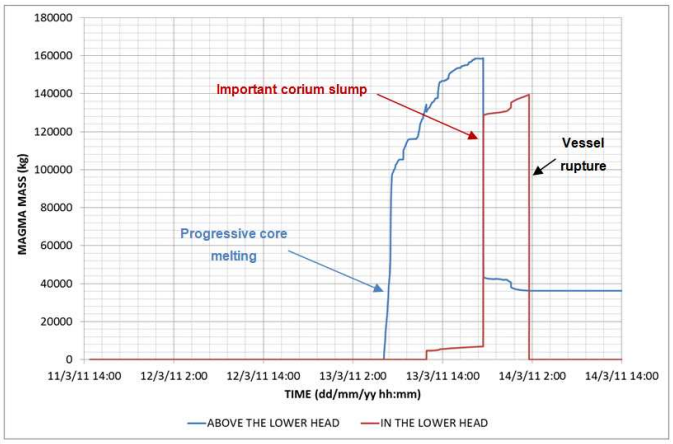

Figure 11. Mass of magma and slump into the lower plenum (kg)

5.2. In-vessel melt composition for Unit 3

As for Unit 2, the analysis is limited to some features – mainly the presence of U – as no exhaustive table for results in the lower head has been generated.
At vessel failure time 52.8 tons of $U0_2$ are located in lower head according to computations and 8.7 tons of U. Those figures are quite similar to the ones observed for Unit 2 however a look at the materials distributions in the layers shows a very different behavior. As for Unit 2, a significant debris layer remains un-molten thanks to the water injections. However, its mass is only about a quarter of the Unit 2 debris layer. Most of the melt is located in the upper layer with only some tons of materials present in the two bottom layers indicating that mass transfers between layers have been weak (see Table III. below for the species distribution in the layers). It has to be linked with the fact that the corium layers are highly cooled.

Table III. 1F3 – Main species distribution in the layers (kg/species/layer)

Species	U	UO_2	Zr	ZrO_2	B_4C	Steel species	Total
Magma 1	129	2560	64	1540	< 1	1377	5670
Magma 2	62	1650	32	994	< 1	42	2780
Magma 3	8520	40900	4490	25700	249	34141	114000

In a whole, as for Unit 2, the quantity of metallic zirconium in the lower head is rather limited, less 5 tons (around 6 tons for Unit 2 with a quite similar slump mass). This may be attributed to the steam provided by the water injections. The ratio between U present as a metal (8.7 tons) and the total mass of U in the magma layers (48.5 tons which includes the 39.8 tons bound in the 45.1 tons of UO_2) is approximately 18.0 % much less than in Unit 2.

As for Unit 2, in case of vessel failure and massive corium slump to the pedestal, most of metallic U should have been re-oxided whereas if large quantity of corium remained in the lower head, metallic U might be expected.

6. CONCLUSIONS

On the three Fukushima units involved in the severe accident, ASTEC predicts that significant masses of metallic U were formed in the lower head corium slumps roughly 10 tons for each unit. In case of vessel failure and large corium slump to the pedestal – which most probably happened with Unit 1, this metallic U may have been largely or totally re-oxidized by steam produced during the MCCI process. In case the melt may have remained partially or in totality inside the vessel as for Unit 2 and 3, a part of the metallic uranium may still be present inside the vessel bottom head depending on the water injection characteristics.

REFERENCES

1. http://fdada.info
2. Asmolov V. G., Bechta S.V., Khabensky V.B., Gusarov V.V., Vishnevsky V.Yu., Degaltsev Yu.A., Abalin S.S., Krushinov E.V., Vitol S.A., Almjashev V.I., Kotova S.Yu., Zagryazkin V.N., Dyakov E.K., Strizhov V.F., Kiselev N.P., 2004. Partitioning of U, Zr and FP between molten oxidic and metallic corium, MASCA seminar, Aix-en-Provence, France, June 10-11, 2004. http://www.oecd-nea.org/nsd/workshops/masca2004/oc/papers/RF_M_Partitioning.pdf
3. Asmolov V. G., Tsurikov D. F., 2004. MASCA project: major activities and results. MASCA seminar, Aix-en-Provence, France, June 10-11, 2004. http://www.oecd-nea.org/nsd/workshops/masca2004/oc/papers/RF_ASM_M_Activities.pdf
4. Bechta S.V., Granovsky V.S., Khabensky V.B., Gusarov V.V., Almiashev V.I., Mezentseva L.P., Krushinov E.V., Kotova S.Yu., Kosarevsky R.A., Barrachin M., Bottomley D., Fichot F., Fischer M., “Corium phase equilibria based on MASCA, METCOR and CORPHAD results”, Nuclear Engineering and Design, 238 (10), pp. 2761-2771 (2008).
5. Jacquemain D., Vola D., Meignen R., Bonnet J.-M., Fichot F., Raimond E., Barrachin M., “Past and future R1D at IRSN on corium progression and related mitigation strategies in a severe accident”. Paper presented in the NURETH-16 congress, Chicago, 2015
6. L.M. Kachanov. Time of the rupture process under creep conditions. *Izv. Akad. Nauk. SSR, Otd Tekh. Nauk.*, 8:26–31, 1958.